Application of the Schwinger variational principle to electron-ion scattering in the static-exchange approximation

Robert R. Lucchese and Vincent McKoy

Arthur Amos Noyes Laboratory of Chemical Physics, * *California Institute of Technology, Pasadena, California 91125*
(Received 9 March 1979)

The authors present a method for applying the Schwinger variational principle to the scattering of low-energy electrons by molecular ions. Numerical procedures for its application in the static-exchange approximation are specifically discussed. As examples, the s- and p-wave phase shifts for e-He$^+$ are obtained. The procedure also provides the electron continuum wave functions which can be used to obtain photoionization cross sections. The resulting cross sections for photoionization of the ground and metastable states of the He are seen to be accurate.

I. INTRODUCTION

In recent years several methods which employ discrete basis sets have been successfully developed to study electron-molecule scattering and photoionization processes in molecules. These methods include the R-matrix method used by Schneider[1-3] for e-H$_2$, N$_2$, and F$_2$ scattering; the T-matrix method introduced by Rescigno, McCurdy, and McKoy,[4,5] and applied to e-H$_2$, N_2, and CO, (Refs. 6-9); and the Stieltjes imaging technique developed by Langhoff[10,11] and applied to photoionization cross sections of molecules including N$_2$, CO, H$_2$O, and H$_2$CO.[12-15]

In the present work, we compute static-exchange electron-ion scattering phase shifts by direct evaluation of the Schwinger variational expression for the K matrix. The Schwinger principle has several distinct advantages over other variational methods. In the Schwinger method the trial function is not required to satisfy any specific asymptotic boundary condition. The method is also not troubled by the spurious singularities that can arise in the Kohn variational method. In the form used here, a trial wave function is constructed from a linear combination of Cartesian Gaussian functions.

The Schwinger variational expression also yields an approximate wave function expressed as a linear combination of discrete basis functions. With little additional computational effort, an improved numerical wave function can be generated using the Lippmann-Schwinger equation in an iterative fashion as suggested by Blatt and Jackson.[16] Thus the present application of the Schwinger principle also yields numerical wave functions with asymptotic forms corresponding to the variationally determined K matrix.

This method is well suited to electron–molecular-ion scattering. The expressions presented in this paper are general for symmetric linear molecules.

As a specific test case we have studied e-He$^+$ scattering. In addition to calculating s- and p-wave phase shifts, the scattering solutions have been used to calculate photoionization cross sections of the $1\,^1S$, $2\,^1S$, and $2\,^3S$ states of helium.

II. THEORY

A. Electon-ion scattering

The Schrödinger equation for potential scattering from a molecular ion of net charge Z is of the form (in atomic units)

$$[-\nabla^2 - 2Z/r + U^s(\vec{r}) - k^2]\psi_{\vec{k}}(\vec{r}) = 0. \tag{1}$$

The potential $U^s(\vec{r})$ is an optical potential representing the short-range interactions between the target and the scattered electron.

Instead of solving the Schrödinger equation directly, the Lippmann-Schwinger equation for the wave function is used. For electron-ion scattering considered here, the Lippmann-Schwinger equation is

$$\psi_{\vec{k}}^{(\pm)} = \psi_{\vec{k}}^{c(\pm)} + G^{c(\pm)}U^s\psi_{\vec{k}}^{(\pm)}, \tag{2}$$

where the Coulomb Green's function is

$$G^{c(\pm)} = (\nabla^2 + 2Z/r + k^2 \pm i\epsilon)^{-1} \tag{3}$$

and $U^s(\vec{r}) = 2V^s(\vec{r})$. The wave function $\psi_{\vec{k}}^{c(\pm)}$, is the pure Coulomb scattering wave function which has the partial-wave expansion given by

$$\psi_{\vec{k}}^{c(\pm)}(\vec{r}) = \left(\frac{2}{\pi}\right)^{1/2} \sum_{lm} i^l e^{\pm i\sigma_l} \frac{F_l(\gamma; kr)}{kr} Y_{lm}(\hat{r})Y_{lm}^*(\hat{k}), \tag{4}$$

where $F_l(\gamma; kr)$ is the regular Coulomb function and

$$\gamma = -Z/k \text{ and } \sigma_l = \arg[\Gamma(l+1+i\gamma)].$$

The partial-wave expansion[17] of the Coulomb Green's function $G^{c(\pm)}$ is

$$G^{c(\pm)}(\vec{r}, \vec{r}') = -\frac{1}{k}\sum_{lm}Y_{lm}(\hat{r})Y^{*}_{lm}(\hat{r}')r^{-1}r'^{-1}$$

$$\times F_l(\gamma; kr_<)$$

$$\times [G_l(\gamma; kr_>) \pm iF_l(\gamma; kr_>)].$$

(5)

The asymptotic form of the scattering solution is then

$$\psi^{(\pm)}_{\vec{k}}(\vec{r}) \sim \psi^{c(\pm)}_{\vec{k}}(\vec{r}) + f^{(\pm)}_{\vec{k}}(\hat{r})\frac{1}{(2\pi)^{3/2}}$$

$$\times \frac{\exp[\pm i(kr - \gamma\,\ln 2kr)]}{r},$$

(6)

where

$$f^{(\pm)}_{\vec{k}}(\hat{r}) = -2\pi^2\langle\psi^{c(\mp)}_{\pm k\hat{r}}|U^s|\psi^{(\pm)}_{\vec{k}}\rangle.$$

(7)

We can define the T matrix due to the short-range component of the potential, U^s, by

$$T^{s(\pm)} = U^s + U^sG^{c(\pm)}T^{s(\pm)}.$$

(8)

It then follows that

$$T^{s(\pm)}|\psi^{c(\pm)}_{\vec{k}}\rangle = U^s|\psi^{(\pm)}_{\vec{k}}\rangle,$$

(9)

and hence

$$f^{(\pm)}_{\vec{k}}(\hat{r}) = -2\pi^2\langle\psi^{c(\mp)}_{\pm k\hat{r}}|T^{s(\pm)}|\psi^{c(\pm)}_{\vec{k}}\rangle.$$

(10)

In actual calculations the principal-value function, defined by

$$\psi^{(P)}_{\vec{k}} = \psi^{c(P)}_{\vec{k}} + G^{c(P)}U^s\psi^{(P)}_{\vec{k}}$$

(11)

is used. We define the partial-wave expansion of the principal-value Coulomb function, $\psi^{c(P)}_{\vec{k}}$, by

$$\psi^{c(P)}_{\vec{k}} = \left(\frac{2}{\pi}\right)^{1/2}\frac{1}{kr}\sum_{lm}i^lF_l(\gamma; kr)Y_{lm}(\hat{r})Y^{*}_{lm}(\hat{k}).$$

(12)

This definition for the principal-value wave function is chosen so that $\psi^{c(P)}_{\vec{k}}$ is normalized to $\delta(k - k')$. The expansion of $\psi^{c(P)}_{\vec{k}}$ in Eq. (12) is similar to that given for $\psi^{c(\pm)}_{\vec{k}}$ in Eq. (4), except that the partial-wave radial functions have been made real, i.e., the factor $e^{\pm i\sigma_l}$ has been dropped.

Defining the K^s matrix by

$$K^s = -\tfrac{1}{2}\pi U^s + U^sG^{c(P)}K^s$$

(13)

with the partial-wave K^s matrix elements given by

$$K^s_{l'lm} = \frac{2k}{\pi}\left\langle\frac{F_{l'}(\gamma; kr)}{kr}Y_{l'm}(\hat{r})\middle|K^s\middle|\frac{F_{lm}(\gamma; kr)}{kr}Y_{lm}(\hat{r})\right\rangle$$

(14)

and the partial-wave expansion of $\psi^{(P)}_{\vec{k}}(\vec{r})$ defined as

$$\psi^{(P)}_{\vec{k}}(\vec{r}) = \left(\frac{2}{\pi}\right)^{1/2}\frac{1}{kr}\sum_{ll'm}i^l\psi^{(P)}_{ll'm}(r)Y_{l'm}(\hat{r})Y^{*}_{lm}(\hat{k}),$$

(15)

we have for the asymptotic form of the partial-wave functions

$$\psi^{(P)}_{ll'm} \sim F_l(\gamma; kr)\delta_{ll'} + G_{l'}(\gamma; kr)K^s_{l'lm}.$$

(16)

The T matrix is related to the K matrix by defining the partial-wave expansion of the on-shell T matrix as

$$\langle\psi^{c(\mp)}_{(\pm\vec{k})}|T^{s(\pm)}|\psi^{c(\pm)}_{\vec{k}}\rangle$$

$$= \frac{1}{k}\sum_{ll'm}i^{l-l'}Y_{l'm}(\pm\hat{k}')T^{s(\pm)}_{l'lm}Y^{*}_{lm}(\hat{k}).$$

(17)

Then $T^{s(\pm)}_{l'lm}$ is given by

$$T^{s(\pm)}_{l'lm} = \frac{2k}{\pi}e^{\pm i(\sigma_{l'} + \sigma_l)}$$

$$\times\left\langle\frac{F_{l'}(\gamma; kr)}{kr}Y_{l'm}(\hat{r})\middle|T^{s(\pm)}\middle|\frac{F_l(\gamma; kr)}{kr}Y_{lm}(\hat{r})\right\rangle.$$

(18)

Now the T matrix can be obtained from the K matrix using

$$T^{s(\pm)}_{l'lm} = -\frac{2}{\pi}e^{\pm i(\sigma_{l'} + \sigma_l)}$$

$$\times\sum_{l''}[(1 \mp iK^s)^{-1}]_{l'l''m}K^s_{l''lm}.$$

(19)

The relation between $\psi^{(P)}_{\vec{k}}$ and $\psi^{(\pm)}_{\vec{k}}$ is then given by

$$\psi^{(\pm)}_{ll'm}(r) = e^{\pm i\sigma_l}\sum_{l''}[(1 \mp iK^s)^{-1}]_{ll''m}\psi^{(P)}_{l''l'm}(r).$$

(20)

The approach taken here to solve the Lippmann-Schwinger equation for the K-matrix is to assume a separable potential of the form

$$\bar{U}^s = \sum_{\alpha,\beta}U^s|\alpha\rangle[d^{-1}]_{\alpha\beta}\langle\beta|U^s,$$

(21)

where $d_{\alpha\beta} = \langle\alpha|U^s|\beta\rangle$. We chose the expansion functions to be Cartesian Gaussian functions of the form

$$\phi^\alpha(\vec{r}) = \langle\vec{r}|\alpha\rangle = N_{lmn}(x - A_x)^l(y - A_y)^m$$

$$\times (z - A_z)^n e^{-\alpha|\vec{r} - \vec{A}|^2}$$

(22)

where $\vec{A}$ locates the basis function center and N_{lmn} is a normalization factor. Substitution of this expression into the Lippmann-Schwinger equation yields

$$\bar{K}^s = -\frac{\pi}{2}\sum_{\alpha\beta}U^s|\alpha\rangle[f^{-1}]_{\alpha\beta}\langle\beta|U^s,$$

(23)

where

$$f_{\alpha\beta} = \langle\alpha|U^s|\beta\rangle - \langle\alpha|U^sG^{c(P)}U^s|\beta\rangle.$$

Adhikari and Sloan[18] have shown that a separable potential of this form in the Lippmann-Schwinger equation yields an expression for the K matrix which is equivalent to the Schwinger variational

expression with trial wave functions expanded in the same bases, e.g.,

$$\psi_{\vec{k}}^{t(P)} = \sum_{\alpha} a_{\alpha}(\vec{k}) \,|\, \alpha\rangle .$$

B. Static-exchange potential for e^--ion scattering

The potential, $U^s(\vec{r})$, used in the present work is just the static-exchange potential. For a two-electron system the electronic wave function is of the form

$$\psi(1, 2) = u'(1)u^0(2) \pm u'(2)u^0(1) , \tag{24}$$

where the upper (lower) sign gives the singlet (triplet) solution. The one-electron orbital u' is taken to be a continuum orbital, and u^0 is fixed as the bound orbital of the isolated one-electron ion. The electronic Hamiltonian for this two-particle system, where the ion is an atomic, homonuclear diatomic, or symmetric linear triatomic system is

$$H(1, 2) = h(1) + h(2) + 1/r_{12} , \tag{25}$$

where

$$h(i) = -\tfrac{1}{2}\nabla_i^2 - \frac{Z_c}{r_i} - Z_A \left(\frac{1}{|\vec{r}_i - \vec{A}|} + \frac{1}{|\vec{r}_i + \vec{A}|} \right)$$

and Z_c and Z_A are the nuclear charges at the origin and at $\vec{A}$ and $-\vec{A}$, respectively.

With the orbital u^0 fixed, the solution of the Schrödinger equation

$$H\psi = E\psi \tag{26}$$

reduces to the one-electron equation for u',[19-21]

$$(h \pm Q^{u^0} \mp \epsilon_0 P^{u^0} + J^{u^0} \pm K^{u^0})u' = \epsilon_1(1 \pm P^{u^0})u' , \tag{27}$$

where the various operators are defined by

$$Q^{u^0}(\vec{r})u'(\vec{r}) = u^0(\vec{r}) \int d^3r' u^{0*}(\vec{r}')h(\vec{r}')u'(\vec{r}')$$
$$+ h(\vec{r})u^0(\vec{r}) \int d^3r' u^{0*}(\vec{r}')u'(\vec{r}') ,$$

$$P^{u^0}(\vec{r})u'(\vec{r}) = u^0(\vec{r}) \int d^3r' u^{0*}(\vec{r}')u'(\vec{r}') , \tag{28}$$

$$J^{u^0}(\vec{r})u'(\vec{r}) = u'(\vec{r}) \int d^3r' \frac{u^{0*}(\vec{r}')u^0(\vec{r}')}{|\vec{r}' - \vec{r}|} ,$$

$$K^{u^0}(\vec{r})u'(\vec{r}) = u^0(\vec{r}) \int d^3r' \frac{u^{0*}(\vec{r}')u'(\vec{r}')}{|\vec{r}' - \vec{r}|} ,$$

and where

$$\epsilon_0 = \int d^3r u^{0*}(\vec{r})h(\vec{r})u_0(\vec{r}) \tag{29}$$

and $\epsilon_1 = E - \epsilon_0$.

When u^0 is an eigenfunction of h, Eq. (27) reduces to

$$(h \pm \epsilon_0 P^{u^0} + J^{u^0} \pm K^{u^0})u' = \epsilon_1(1 + P^{u^0})u' . \tag{30}$$

In the triplet case Eq. (30) is equivalent to the simpler equation

$$(h + J^{u^0} - K^{u^0})u' = \epsilon_1 u' , \tag{31}$$

since the solutions to Eq. (30) are just an arbitrary linear combination of u^0 and the solutions to Eq. (31).[19,22] Thus the solutions to Eq. (3) are constrained to be orthogonal to the occupied bound orbital, u^0, where the solutions of Eq. (30) have no such orthogonality constraint imposed on them.

The potential in the static-exchange approximation is then

$$U^s(\vec{r}) = 2[N^{\vec{A}}(\vec{r}) + J^{u^0} \pm (K^{u^0} + Q^{u^0})$$
$$\mp (\epsilon_0 + \tfrac{1}{2}k^2)P^{u^0}] , \tag{32}$$

where

$$N^{\vec{A}}(\vec{r}) = -\frac{Z_c - Z}{r} - Z_A \left(\frac{1}{|\vec{r} - \vec{A}|} + \frac{1}{|\vec{r} + \vec{A}|} \right) . \tag{33}$$

Note that this potential is momentum dependent, although all of the individual operators are independent of momentum. The corresponding potential in the case where u^0 is an eigenfunction of h is

$$U^s(\vec{r}) = 2[N^{\vec{A}}(\vec{r}) + J^{u^0} \pm K^{u^0} \pm (\epsilon_0 - \tfrac{1}{2}k^2)P^{u^0}] . \tag{34}$$

In the triplet case the potential for the solution which is constrained to be orthogonal to the bound orbital is given by

$$U^s(\vec{r}) = 2[N^{\vec{A}}(\vec{r}) + J^{u^0} - K^{u^0}] . \tag{35}$$

III. IMPLEMENTATION

A. Matrix elements

There are three types of matrix elements needed to evaluate the parital-wave K-matrix elements by the Schwinger variational principle:

$$\bar{K}_{ll'm}^s = -k \sum_{\alpha,\beta} \left\langle \frac{F_{l'}(\gamma; kr)}{kr} Y_{l'm}(\hat{r}) \,\middle|\, U^s \,\middle|\, \alpha \right\rangle [f^{-1}]_{\alpha\beta}$$
$$\times \left\langle \beta \,\middle|\, U^s \,\middle|\, \frac{F_l(\gamma; kr)}{kr} Y_{lm}(\hat{r}) \right\rangle , \tag{36}$$

where $[f^{-1}]_{\alpha\beta}$ is obtained by inverting the matrix with elements

$$f_{\alpha\beta} = \langle \alpha \,|\, U^s \,|\, \beta \rangle - \langle \alpha \,|\, U^s G^{c(P)} U^s \,|\, \beta \rangle . \tag{37}$$

The elements of the type $\langle \alpha \,|\, U^s \,|\, \beta \rangle$ are available from standard bound-state molecular integral programs. The other two types of matrix elements

$$\left\langle \alpha \,\middle|\, U^s \,\middle|\, \frac{F_l(\gamma; kr)}{kr} Y_{lm}(\hat{r}) \right\rangle \text{ and } \langle \alpha \,|\, U^s G^{c(P)} U^s \,|\, \beta \rangle$$

are evaluated directly by numerical integration.

The initial step in the numerical procedure is to compute $U^\alpha(\vec{r}) = \langle \vec{r} \,|\, U^s \,|\, \alpha \rangle$. This is done by first partial-wave expanding the Cartesian Gaussian functions with

$$\phi^\alpha(\vec{r}) = \sum_{lm} \frac{\phi_{lm}^\alpha(r)}{r} Y_{lm}(\hat{r}). \qquad (38)$$

These expansions are analytically known.[23] Then we define the partial-wave expansion of the potential by

$$U^\alpha(\vec{r}) = \sum_{lm} \frac{U_{lm}^\alpha(r)}{r} Y_{lm}(\hat{r}). \qquad (39)$$

In turn each operator which contributes to U^s can be similarly expanded.

For the case where the occupied orbital u^0 is of $\sigma(m = 0)$ symmetry, it has the partial-wave expansion

$$u^0(\vec{r}) = \sum_l \frac{u_l^0(r)}{r} Y_{l0}(\hat{r}). \qquad (40)$$

Then the expansions of the operators J, K, and N are[23]

$$J_{lm}^{u^0, \alpha}(r) = \sum_{l'=0}^{\infty} \left(\frac{2l+1}{2l'+1}\right)^{1/2} \sum_{\lambda=0}^{\infty} (l\lambda 00 \,|\, l'0)(l\lambda m0 \,|\, l'm)$$
$$\times \phi_{l'm}^\alpha(r) V_\lambda(r), \qquad (41)$$

where

$$V_\lambda(r) = \sum_{s,s'=0}^{\infty} \frac{[(2s+1)(2s'+1)]^{1/2}}{2\lambda+1} (ss'00 \,|\, \lambda 0)^2 \left(\frac{1}{r^{\lambda+1}} \int_0^r dr' \, u_s^{0*}(r') u_{s'}^0(r') r'^\lambda \right.$$
$$\left. + r^\lambda \int_r^\infty dr' \, u_s^{0*}(r') u_{s'}^0(r') r'^{-\lambda-1} \right), \qquad (42)$$

$$K_{lm}^{u^0, \alpha}(r) = \sum_{l'=0}^{\infty} \sum_{s,s',\lambda=0}^{\infty} A^0(l, l', m; s, s', \lambda) u_{s'}^0(r) \left(\frac{1}{r^{\lambda+1}} \int_0^r dr' \, u_s^{0*}(r') \phi_{l'm}^\alpha(r') r'^\lambda \right.$$
$$\left. + r^\lambda \int_r^\infty dr' \, u_s^{0*}(r') \phi_{l'm}^\alpha(r') r'^{-\lambda-1} \right), \qquad (43)$$

$$A^0(l, l', m; s, s', \lambda) = \left(\frac{(2s+1)(2s'+1)}{(2l+1)(2l'+1)}\right)^{1/2} (s\lambda 00 \,|\, l'0)(s'\lambda 00 \,|\, l0)(s\lambda 0m \,|\, l'm)(s'\lambda 0m \,|\, lm), \qquad (44)$$

and

$$N_{lm}^{\vec{A}, \alpha}(r) = \sum_{l'=0}^{\infty} \left(\frac{2l+1}{2l'+1}\right)^{1/2} \sum_{\lambda=0}^{\infty} (l\lambda 00 \,|\, l'0)(l\lambda m0 \,|\, l'm) \left[-2Z_A \left(\frac{r_<^\lambda}{r_>^{\lambda+1}}\right)_A - \delta_{\lambda,0}\left(\frac{Z_c - Z}{r}\right)\right] \phi_{l'm}^\alpha(r), \qquad (45)$$

with

$$(r_<^\lambda / r_>^{\lambda+1})_A = \begin{cases} A^\lambda / r^{\lambda+1}, & A < r \\ r^\lambda / A^{\lambda+1}, & A > r \end{cases} \qquad (46)$$

and $\vec{A} = A\hat{z}$. The quantities $(j_1 j_2 m_1 m_2 \,|\, j_3 m_3)$ are Clebsch-Gordan coefficients. The expansions for the operators Q and P are

$$P_{l0}^{u^0, \alpha}(r) = \langle u^0 \,|\, \alpha \rangle u_{lm}^0(r) \qquad (47)$$

and

$$Q_{lm}^{u^0, \alpha}(r) = \langle u^0 \,|\, h \,|\, \alpha \rangle u_{lm}^0(r)$$
$$+ \langle u^0 \,|\, \alpha \rangle \left[-\frac{1}{2}\frac{d^2}{dr^2} + \frac{l(l+1)}{2r^2} - 2Z_A \left(\frac{r_<^\lambda}{r_>^{\lambda+1}}\right)_A \right.$$
$$\left. - \delta_{l,0}\frac{Z_c}{r}\right] u_{lm}^0(r). \qquad (48)$$

In general $u^0(\vec{r})$ is also a linear combination of Cartesian Gaussian functions. Thus the integrals $\langle u^0 \,|\, \alpha \rangle$ and $\langle u^0 \,|\, h \,|\, \alpha \rangle$ as well as the expansions $u_{ln}^0(r)$ are evaluated analytically. The expanded potential is then given by

$$U_{lm}^\alpha(r) = 2\{N_{lm}^{\vec{A}, \alpha}(r) + J_{lm}^{u^0, \alpha}(r)$$
$$\pm [K_{lm}^{u^0, \alpha}(r) + Q_{lm}^{u^0, \alpha}(r)]$$
$$\mp (\epsilon_0 + \tfrac{1}{2}k^2) P_{lm}^{u^0, \alpha}(r)\}. \qquad (49)$$

The hybrid integrals are evaluated using

$$\left\langle \alpha \,\middle|\, U^s \,\middle|\, \frac{F_l(\gamma; kr)}{kr} Y_{lm}(\hat{r}) \right\rangle = \frac{1}{k} \int_0^\infty dr \, F_l(\gamma; kr) U_{lm}^\alpha(r). \qquad (50)$$

Finally the matrix element $\langle \alpha \,|\, U^s G^{c\,(P)} U^s \,|\, \beta \rangle$ in the denominator of Eq. (36) is given by

$$\langle \alpha \,|\, U^s G^{c\,(P)} U^s \,|\, \beta \rangle = -\frac{1}{k} \sum_{lm} \int_0^\infty dr \, U_{lm}^\alpha(r) \left(G_l(\gamma; kr) \int_0^r dr' \, U_{lm}^\beta(r') F_l(\gamma; kr') \right.$$
$$\left. + F_l(\gamma; kr) \int_r^\infty dr' \, U_{lm}^\beta(r') G_l(\gamma; kr') \right). \qquad (51)$$

B. Electron-ion scattering wave functions

Numerical wave functions are generated from the K matrix using the method of Fliflet and Mc-Koy.[8] The identity

$$U^s|\psi_{\underset{k}{\pm}}^{(P)}\rangle = -(2/\pi)K^s|\psi_{\underset{k}{c}}^{(P)}\rangle \qquad (52)$$

combined with Eq. (1), yields

$$\left(-\frac{d^2}{dr^2} + \frac{l(l+1)}{r^2} - \frac{2Z}{r} - k^2\right)\psi_{ll'm}^{(P)}(r)$$

$$= +\frac{2k}{\pi}\left\langle Y_{l'm}(\hat{r})|K^s\left|\frac{F_{lm}(\gamma; kr)}{kr}Y_{lm}(\hat{r})\right\rangle. \quad (53)$$

In the present formulation the right-hand side of Eq. (53) is approximated by

$$\frac{2k}{\pi}\left\langle Y_{l'm}(\hat{r})|\tilde{K}^s\left|\frac{F_{lm}(\gamma; kr)}{kr}Y_{lm}(\hat{r})\right\rangle\right.$$

$$= -k\sum_{\alpha,\beta}U_{l'm}^{\alpha}(r)[f^{-1}]_{\alpha\beta}$$

$$\times\left\langle\beta|U^s\left|\frac{F_{lm}(\gamma; kr)}{kr}Y_{lm}(\hat{r})\right\rangle. \quad (54)$$

These uncoupled ordinary differential equations are easily solved using the Numerov method subject to the boundary conditions[8]

$$\lim_{r\to 0}\psi_{ll'm}^{(P)}(r) = 0 \qquad (55a)$$

$$\lim_{r\to\infty}\psi_{ll'm}^{(P)}(r) = F_l(\gamma; kr)\delta_{ll'}$$

$$+ \tilde{K}_{l'lm}^s G_{l'}(\gamma; kr). \qquad (55b)$$

This prescription for generating numerical wave functions is equivalent to the iterative use of the Lippmann-Schwinger equation suggested by Blatt and Jackson.[16] For a given trial wave function $\psi_{\underset{k}{\overset{t}{}}}^{(P)}$ they suggested that it could be improved by using

$$\psi_{\underset{k}{\overset{t'}{}}}^{(P)} = \psi_{\underset{k}{\overset{c}{}}}^{(P)} + G^{c(P)}U^s\psi_{\underset{k}{\overset{t}{}}}^{(P)}. \qquad (56)$$

Thus the solution of Eqs. (53) and (54) is identical to the solution of Eq. (56) with the trial function $\psi_{\underset{k}{\overset{t}{}}}^{(P)}$ being given by

$$\psi_{\underset{k}{\overset{t}{}}}^{(P)} = \sum_{\alpha,\beta}\phi^{\alpha}(\vec{r})[f^{-1}]_{\alpha\beta}\langle\beta|U^s|\psi_{\underset{k}{\overset{c}{}}}^{(P)}\rangle, \qquad (57)$$

which is the trial wave function implied by the Schwinger variational expression given in Eq. (36).[18]

C. Photoionization cross sections

In the present work, the electron-ion scattering solutions are also used to calculate photoionization cross sections. Photoionization from three initial states of helium are considered. The states are the ground state $1\,^1S$ and two metastable states $2\,^1S$ and $2\,^3S$.

The initial states in these calculations are of the functional form

$$\psi_i(1,2) = \frac{1}{[2(1\pm S)]^{1/2}}[\phi_{ns'}(1)\phi_{1s}(2)\pm\phi_{1s}(1)\phi_{ns'}(2)],$$

$$(58)$$

where $S = \langle ns'|1s\rangle$. In the $1\,^1S$ calculation, $\phi_{ns'}$ and ϕ_{1s} are the same and are equal to the Hartree-Fock orbital of the ground state of helium in the basis set used. For the two metastable states, ϕ_{1s} is constrained to be the same as in the ground state. The $\phi_{ns'}$ functions are then eigenfunctions of the one-electron equation given in Eq. (27).

The final states used in the photoionization calculation are constructed from the solution of the electron-ion scattering problem where the bound orbital is fixed as the ϕ_{1s} of the ground state. Hence the final orbital is the frozen core of the target. We measure all energies relative to the experimental ionization potentials and in this way compensate for some errors in the frozen-core model. Thus the final states are of the form

$$\psi_{f,\vec{k}}(1,2) = (\tfrac{1}{2}k)^{1/2}[\phi_{1s}(1)\psi_{\underset{k}{(-)}}(2)\pm\psi_{\underset{k}{(-)}}(1)\phi_{1s}(2)].$$

$$(59)$$

The differential dipole oscillator strength is then computed in either the length or velocity form as

$$\left(\frac{df}{dE}\right)_L = \sum_{\mu}\frac{2}{3}\Delta E\int d\Omega_{\hat{k}}|\langle\psi_i|r_{\mu}|\psi_{f,\vec{k}}\rangle|^2 \qquad (60)$$

or

$$\left(\frac{df}{dE}\right)_V = \sum_{\mu}\frac{2}{3}\frac{1}{\Delta E}\int d\Omega_{\hat{k}}|\langle\psi_i|\nabla_{\mu}|\psi_{f,\vec{k}}\rangle|^2, \qquad (61)$$

where $\Delta E = \tfrac{1}{2}k^2 + \text{IP}$ and

$$r_{\mu} = \begin{cases} \mp(x\pm iy)/\sqrt{2} & \text{for } \mu=\pm 1 \\ z & \text{for } \mu=0 \end{cases} \qquad (62)$$

and

$$\nabla_{\mu} = \begin{cases} \mp\left(\dfrac{\partial}{\partial x}\pm i\dfrac{\partial}{\partial y}\right)\Big/\sqrt{2} & \text{for } \mu=\pm 1 \\ \dfrac{\partial}{\partial z} & \text{for } \mu=0. \end{cases} \qquad (63)$$

If p_{μ} stands for either r_{μ} or ∇_{μ}, then since all bound orbitals are of gerade symmetry,

$$\langle\psi_i|p_{\mu}|\psi_{f,\vec{k}}\rangle$$

$$= \left(\frac{k}{1\pm S}\right)^{1/2}[S\langle\phi_{1s}|p_{\mu}|\psi_{\underset{k}{(-)}}\rangle\pm\langle\phi_{ns'}|p_{\mu}|\psi_{\underset{k}{(-)}}\rangle]. \quad (64)$$

The bound orbital ϕ (either ϕ_{1s} or $\phi_{ns'}$) has the partial-wave expansion

$$\phi(\vec{r}) = \sum_{lm}\frac{\phi_{lm}(r)}{r}Y_{lm}(\hat{r}), \qquad (65)$$

then

$$\langle\phi|p_\mu|\psi_{\vec{k}}^{(-)}\rangle=\left(\frac{2}{\pi}\right)^{1/2}\frac{1}{k}\sum_{lm}i^lY_{lm}^*(\hat{k})e^{-i\sigma_l}\sum_{l'}[(1+iK)^{-1}]_{ll'm}\sum_{l''l'''m'}\left\langle\frac{\phi_{l''m''}}{r}(r)Y_{l''m''}(\hat{r})\Big|p_\mu\Big|\frac{\psi_{l'l'''m}^{(P)}}{r}(r)Y_{l'''m}(\hat{r})\right\rangle.$$

(66)

The integral on the right-hand side of Eq. (66) in the length form is

$$\left\langle\frac{\phi_{l''m''}}{r}(r)Y_{l''m''}(\hat{r})|r_\mu|\frac{\psi_{l'l'''m}^{(P)}}{r}(r)Y_{l'''m}(\hat{r})\right\rangle=C(l'',l''',m'',m,\mu)\int_0^\infty dr\,\phi_{l''m''}^*(r)r\psi_{l'l'''m}^{(P)}(r),$$

(67)

where

$$C(l'',l''',m'',m,\mu)=\left(\frac{2l'''+1}{2l''+1}\right)^{1/2}(1l'''00|l''0)(1l'''\mu m|l''m'').$$

(68)

In the velocity form the integral in Eq. (66) is given by[24]

$$\left\langle\frac{\phi_{l''m''}(r)}{r}Y_{l''m''}(\hat{r})\Big|\nabla_\mu\Big|\frac{\psi_{l'l'''m}^{(P)}(r)}{r}Y_{l'''m}(\hat{r})\right\rangle$$

$$=C(l'',l''',m'',m,\mu)\int_0^\infty dr\,\phi_{l''m''}^*(r)\left(\frac{d}{dr}+\frac{l'''(l'''+1)-l''(l''+1)}{2r}\right)\psi_{l'l'''m}^{(P)}(r).$$

(69)

IV. RESULTS

A. e^--He$^+$ phase shifts

The first application of the method presented here is to e^--He$^+$ scattering. The He$^+$ target 1s orbital is constructed from the Huzinaga hydrogen 10s basis set[25] with the exponents scaled up by a factor of 2. This basis set gives an energy of $-1.999\,985$ a.u. for He$^+$.

We perform the scattering calculation using three different methods. Besides the exact Schwinger method, we also computed an approximate form of the Schwinger expression as proposed by Watson and McKoy,[26] where the denominator $f_{\alpha\beta}$ is approximated

$$f_{\alpha\beta}^I=\langle\alpha|U^s|\beta\rangle-\sum_{\gamma,\delta}\langle\alpha|U^s|\gamma\rangle\langle\gamma|G^{c(P)}|\delta\rangle$$
$$\times\langle\delta|U^s|\beta\rangle.$$

(70)

A test of the accuracy of the approximation in Eq. (70) is important since this procedure is particularly attractive for molecular applications. The Schwinger K matrix with this approximation is then given by

$$\tilde{K}^{I(s)}=-\frac{\pi}{2}\sum_{\alpha\beta}U^s|\alpha\rangle[(f^I)^{-1}]_{\alpha\beta}\langle\beta|U^s.$$

(71)

In these calculations the basis set inserted in $U^sG^{c(P)}U^s$ is the same set as is used in the rest of the scattering calculation. The third method is the uncorrected T-matrix method originally proposed by Rescigno, McCurdy, and McKoy.[4,5] In this method the K matrix is calculated using

$$K^{T(s)}=-\frac{\pi}{2}\sum_{\alpha\beta\gamma\delta}|\alpha\rangle\langle\alpha|U^s|\beta\rangle[(f^I)^{-1}]_{\beta\gamma}$$
$$\times\langle\gamma|U^s|\delta\rangle\langle\delta|.$$

(72)

The basis sets used in the exact Schwinger method and the approximate Schwinger method with insertion are given in Table I. The basis sets used in the T-matrix calculations with Eq. (72) are given in Table II.

Results for ^3S scattering, where the scattering solution is constrained to be orthogonal to the bound orbital, are presented in Table III. It is

TABLE I. Exponents for Cartesian Gaussian functions used in Schwinger variational calculations.

5s and 5p sets	3s set	1p set
100.0	100.0	0.500
21.1	4.47	
4.47	0.200	
0.946		
0.200		

TABLE II. Exponents for Cartesian Gaussian functions used in uncorrected T-matrix calculations [Eq. (72)].

10s	10p	20s	
400.0	200.0	537.0	3.86
172.0	92.8	328.0	2.36
73.9	43.1	200.0	1.44
31.7	20.0	122.0	0.879
13.6	9.28	74.6	0.537
5.86	4.31	45.5	0.328
2.52	2.00	27.8	0.200
1.08	0.928	17.0	0.122
0.465	0.431	10.4	0.0746
0.200	0.200	6.32	0.0455

TABLE III. Phase shifts for triplet-s-wave scattering of helium ion.[a]

Momentum k	Schwinger[b] $\tilde{\delta}(5s)$	Schwinger[c] $\tilde{\delta}(3s)$	Approximate[d] Schwinger $\delta^I(5s)$	T matrix[e] $\delta^T(5s)$	T matrix[f] $\delta^T(10s)$	Numerical[g] δ^N
0.1	0.919	0.889	0.920	0.933	0.921	($k=0$, $\delta^N=0.920$)
0.3	0.910	0.880	0.913	0.918	0.910	⋯
0.491	0.893	0.865	0.903	0.894	0.893	0.893
0.779	0.855	0.828	0.883	0.855	0.861	0.855
1.076	0.802	0.780	0.851	0.827	0.816	0.802
1.353	0.747	0.731	0.803	0.812	0.758	0.748
1.897	0.642	0.637	0.673	0.759	0.646	0.645
2.198	0.591	0.590	0.603	0.703	0.611	0.604

[a] Phase shifts are for scattering solutions which are constrained to be orthogonal to the bound orbital, using the potential given by Eq. (35).

[b] Exact Schwinger variational phase shifts [Eq. (23)], for $5s$ basis set given in Table I.

[c] Exact Schwinger variational phase shifts for $3s$ basis set given in Table I.

[d] Approximate Schwinger variational phase shifts, with insertion in the denominator [Eq. (71)], for $5s$ basis set given in Table I.

[e] Uncorrected T-matrix phase shifts [Eq. (72)] for $5s$ basis set given in Table I.

[f] Uncorrected T-matrix phase shifts for $10s$ basis set given in Table II.

[g] Phase shifts of numerical solution of Schrödinger equation from Ref. 28.

well known[18,19] that for triplet scattering this yields the same phase shift as the solution in which orthogonality is not imposed. The $5s$ Schwinger results are in excellent agreement with the numerical results of Sloan.[27,28] The $3s$ Schwinger phase shifts are within 3% of the correct values. The $3s$ phase shifts also smoothly approach the accurate phase shifts at higher momentum. The approximate Schwinger calculations with insertion in the denominator give very good results at low momentum but at higher momentum show discrepancies of up to 7%. Naturally the results of the Schwinger method in which the $U^s G^{c\,(P)} U^s$ term is evaluated approximately, i.e., with insertion, can be improved by using a larger basis set around $G^{c\,(P)}$. Uncorrected results using the T-matrix equation [Eq. (72)] are presented for two basis sets. The

$5s$ set which was also used in the two Schwinger calculations yields generally poor uncorrected T-matrix results except for energies around $k=0.6$, as can be seen in Fig. 1. The $10s$ basis set gives much better T-matrix phase shifts, which differ from the exact values by less than 2%.

The results for the ^3S e^--He$^+$ scattering calculations in which the scattering function is not constrained to be orthogonal to the bound orbital, are given in Table IV. It can be seen that the $5s$ Schwinger phase shifts are again in good agreement with the numerical values, and they are almost identical to the phase shifts obtained from the constrained ^3S scattering solution. However, the uncorrected T-matrix $10s$ results are dramatically worse than in the constrained calculation. A larger $20s$ basis set does yield T-matrix

TABLE IV. Phase sifts for triplet-s-wave scattering of helium ion.[a]

Momentum k	Schwinger $\tilde{\delta}(5s)$	T matrix $\delta^T(10s)$	T matrix $\delta^T(20s)$	Numerical[b] δ^N
0.1	0.918	0.930	0.920	($k=0$, $\delta^N=0.920$)
0.3	0.909	0.911	0.916	⋯
0.491	0.893	0.964	0.907	0.893
0.779	0.855	1.334	0.854	0.855
1.076	0.802	1.332	0.809	0.802
1.353	0.747	0.998	0.750	0.748
1.897	0.641	0.750	0.645	0.645
2.198	0.590	0.910	0.605	0.604

[a] Phase shifts are for scattering solutions which are not constrained to be orthogonal to the bound orbital, using the potential given by Eq. (32).

[b] Numerical phase shifts from Ref. 28.

TABLE V. Phase shifts for singlet-s-wave scattering of helium ion.

Momentum k	Schwinger $\tilde{\delta}(5s)$	T matrix $\delta^T(10s)$	Numerical[a] δ^N
0.1	0.386	0.400	($k=0$, $\delta^N=0.387$)
0.3	0.378	0.388	...
0.491	0.366	0.361	0.366
0.779	0.341	0.341	0.341
1.076	0.317	0.325	0.318
1.353	0.302	0.314	0.302
1.897	0.290	0.289	0.290
2.198	0.290	0.289	0.283

[a] Numerical phase shifts from Ref. 28.

phase shifts which are again in close agreement with the accurate results.

The results for ^1S scattering are presented in Table V. In this case, the Schwinger $5s$ and $10s$ T-matrix calculations both agree well with Sloan's results.[27,28]

Phase shifts for ^1P scattering are given in Table VI. In this symmetry the exact Schwinger and the approximate Schwinger (with insertion) expressions both give results in close agreement with the static-exchange phase shifts given by McGreevy and Stewart.[29] Results for ^3P scattering are given in Table VII. Again the Schwinger $5p$ and uncorrected $10p$ T-matrix phase shifts are in close agreement.

B. Photoionization cross sections

The initial state used in the ground-state photoionization calculation of helium is constructed from the $10s$ Gaussian set of Huzinaga[25] (also listed in Table VIII), which has a Hartree-Fock energy $E = -2.861\,669$ a.u. For the two metastable states the $10s$ basis set is augmented by seven diffuse basis functions given in Table VIII. The orbital
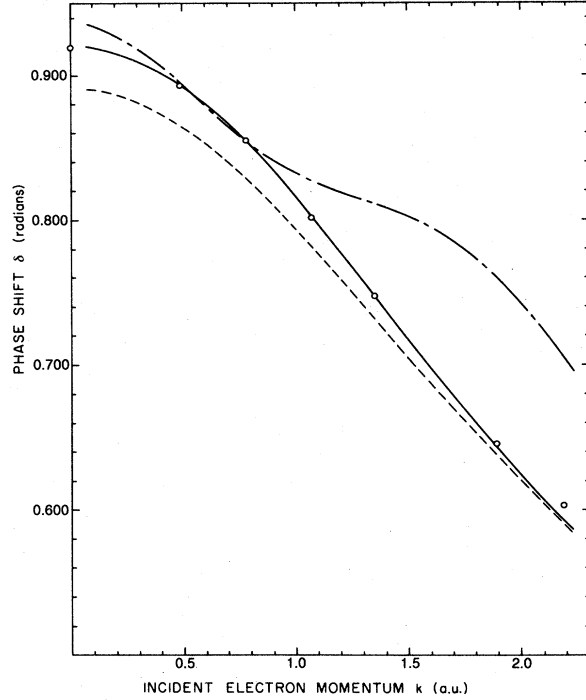

FIG. 1. Comparison of ^3S phase shifts of helium ion, where the scattering solution is constrained to be orthogonal to the bound orbital: solid line, exact Schwinger variational phase shifts with $5s$ basis set given in Table I; dashed line, exact Schwinger variational phase shifts with $3s$ basis set given in Table I; long-dash–short-dashed line, uncorrected T-matrix phase shifts with $5s$ basis set given in Table I; O, numerical phase shifts given by Sloan (Ref. 28).

eigenvalues of the ϕ_{2s}, orbitals, with the ϕ_{1s} orbital taken as the Hartree-Fock orbital, are $-0.141\,509$ a.u. for the $2\,^1S$ state and $-0.189\,942$ a.u. for the $2\,^3S$ state. The more diffuse functions included in this extended basis set are important in describing the Rydberg-like metastable states.

TABLE VI. Phase shifts for singlet-p-wave scattering of helium ion.

Momentum k	Schwinger $\tilde{\delta}(5p)$	Approximate Schwinger $\tilde{\delta}^I(5p)$	T matrix $\delta^T(5p)$	T matrix $\delta^T(10p)$	Numerical[a] δ^N
0.2	−0.0742	−0.0739	−0.0711	−0.0740	−0.0745
0.4	−0.0765	−0.0761	−0.0755	−0.0759	−0.0765
0.6	−0.0788	−0.0783	−0.0782	−0.0742	−0.0788
0.8	−0.0797	−0.0792	−0.0761	−0.0701	−0.0796
1.0	−0.0780	−0.0777	−0.0700	−0.0685	−0.0778
1.2	−0.0733	−0.0732	−0.0633	−0.0690	−0.0727
1.4	−0.0656	−0.0658	−0.0579	−0.0646	−0.0646
1.6	−0.0551	−0.0555	−0.0524	−0.0508	−0.0540

[a] Numerical phase shifts from Ref. 29.
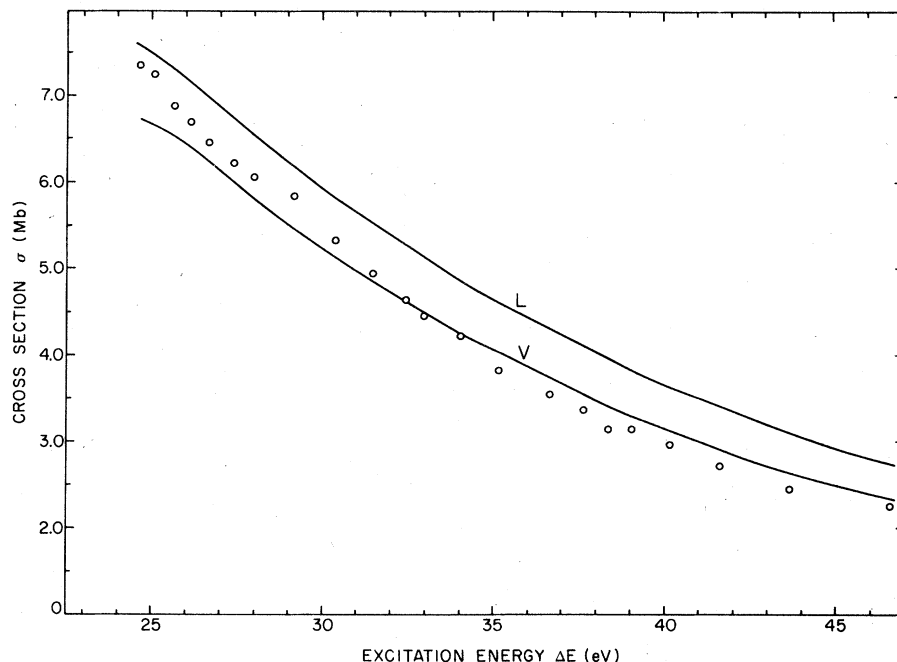
FIG. 2. Photoionization cross sections of $1\,^1S$ He in megabarns: L, static-exchange dipole length; V, static-exchange dipole velocity; $\bigcirc$, selected experimental cross sections from Samson (Ref. 30).

Results of photoionization cross section calculations for the $1\,^1S$ state are presented in Table IX. Cross sections computed using all three methods employed in the scattering calculations are given. The ionization potential is taken to be 0.9035 a.u. (24.59 eV) for the ground state.[30] The exact Schwinger results and approximate Schwinger results, with insertion in the denominator, are virtually identical. These results show that the total cross section is fairly insensitive to the variations in the accuracy of the continuum wave function generated by these various methods. This point is exemplified by the exact Schwinger $1p$ cross sections presented in Table X. The difference between the $1p$ and $5p$ Schwinger cross sections is less than 1%. This result is put into perspective by comparing it to the cross section obtained by

using a pure Coulomb wave as the continuum functions in the final state. The $1p$ results can be seen to be an improvement over the pure Coulomb result which contains no short-range scattering information.

In Fig. 2 the cross sections obtained from an exact Schwinger variational calculation with the $5p$ basis given in Table I, are compared with experimental data given by Samson.[30] The difference

TABLE VII. Phase shifts for triplet-p-wave scattering of helium ion.

Momentum k	Schwinger $\delta(5p)$	T matrix $\delta^T(10p)$
0.2	0.179	0.179
0.4	0.186	0.189
0.6	0.196	0.204
0.8	0.205	0.217
1.0	0.212	0.220
1.2	0.216	0.218
1.4	0.217	0.219
1.6	0.216	0.223

TABLE VIII. Exponents for Cartesian Gaussian functions used in initial-state wave functions.

Huzinaga 10s basis set [a]	Additional diffuse functions for metastable states [b]
3293.694	0.060 0
488.894 1	0.033 3
108.772 3	0.018 5
30.179 9	0.010 3
9.789 053	0.005 71
3.522 261	0.003 17
1.352 436	0.001 76
0.552 610	
0.240 920	
0.107 951	

[a] This is the basis set, from Ref. 25, used in the $1\,^1S$ ($1s^2$) ground state of helium.
[b] The wave functions of the $2\,^1S$ and $2\,^3S$ ($1s2s$) metastable state of helium are constructed from the combined $17s$ basis set.

TABLE IX. Photoionization cross sections of the ground state of helium, using the length form of the dipole operator in megabarns (10^{-18} cm^2).

ΔE (eV)	Schwinger [a] $\tilde{\sigma}(5p)$	Approximate Schwinger [b] $\tilde{\sigma}^I(5p)$	T matrix [c] $\sigma^T(5p)$	T matrix [d] $\sigma^T(10p)$
24.75	7.59	7.59	7.61	7.54
26.6	6.98	6.98	7.07	7.01
30.6	5.76	5.76	5.91	5.83
34.6	4.74	4.75	4.85	4.76
38.6	3.93	3.93	3.95	3.89
42.6	3.26	3.26	3.23	3.22
46.6	2.73	2.73	2.66	2.71

[a] The exact Schwinger photoionization cross section is computed using Eqs. (60), (64), (66), and (67), with the partial-wave scattering solution, $\psi^{(P)}_{ll'm}(r)$, obtained from Eqs. (53) and (54) as described in the text. The $5p$ basis set given in Table I is used.

[b] The approximate Schwinger cross sections are obtained as in footnote (a) except that K^s in Eq. (53) is approximated by $\tilde{K}^{I(s)}$ given in Eq. (71).

[c] The uncorrected T-matrix cross sections are obtained as in footnote (a) except that K^s in Eq. (53) is approximated by $K^{T(s)}$ given in Eq. (72).

[d] Same calculation as in (c) except the $10p$ set given in Table II is used.

between the two forms of the dipole cross section, the length and velocity forms, can be used as an estimate of correlation effects.[31] In the photoionization of the ground state of helium, the static-exchange velocity form yields cross sections closer to the experimental results than does the length form.

The photoionization cross sections of the two metastable states of He, the 2 ^{1}S and 2 ^{3}S states, are shown in Figs. 3 and 4, respectively. The ionization potentials of these states are taken to be 0.145 95 a.u. (3.97 eV) for the 2 ^{1}S state and 0.175 24 a.u. (4.77 eV) for the 2 ^{3}S state.[32] The static-exchange cross sections are compared to the calculated values of Norcross.[33] The calculations by Norcross used close-coupling final-state wave functions with three states included in the expansion. The initial states used by Norcross[33] were slightly different from ours, in that he used a He$^+$ 1s hydrogenic function for the frozen ϕ_{1s} orbital.
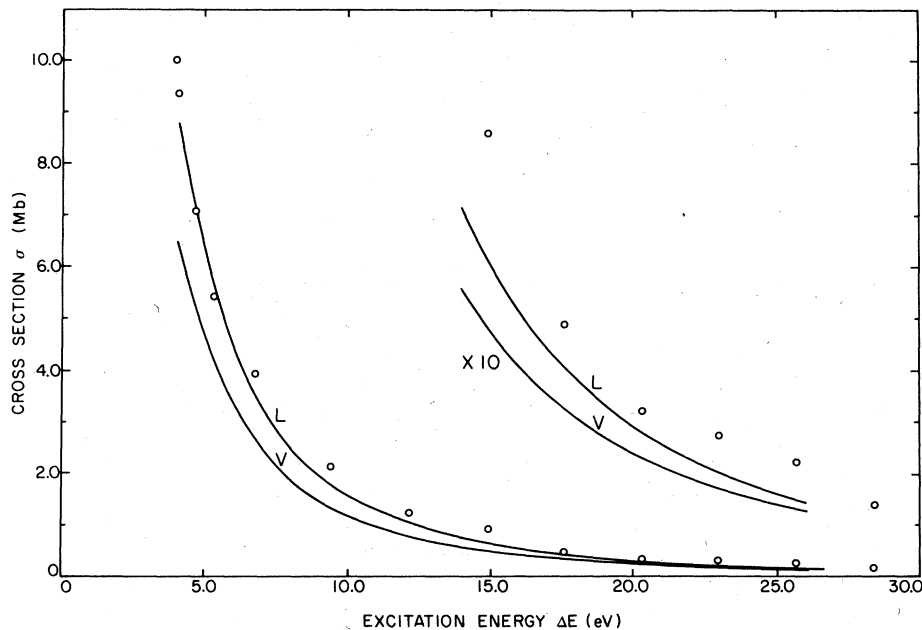

FIG. 3. Photoionization cross sections of 2^{1}S He in megabarns: L, static-exchange dipole length; V, static-exchange dipole velocity; O, numerical results of Norcross (Ref. 33).
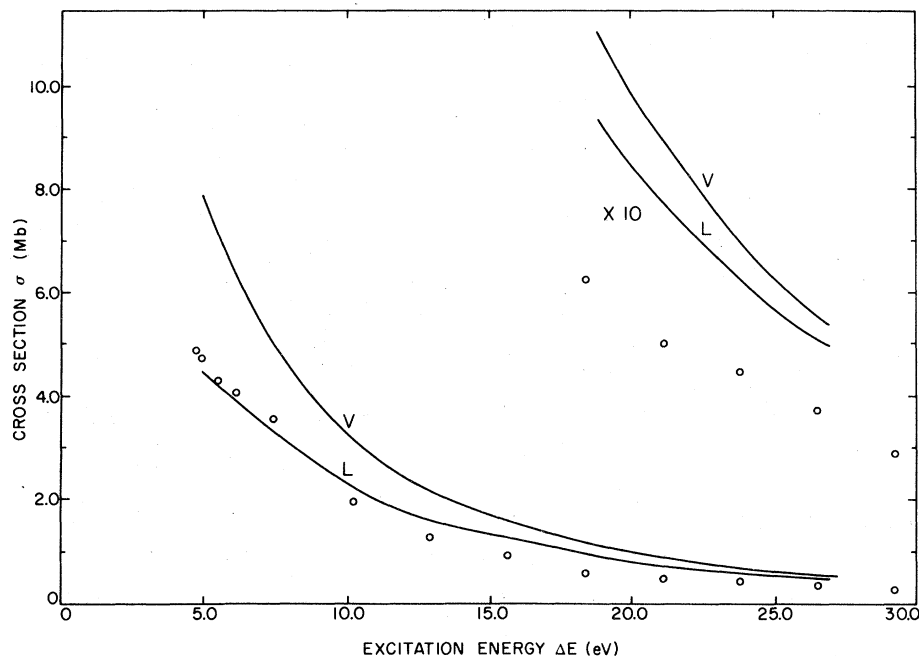
FIG. 4. Photoionization cross sections of $2\,^3S$ He in megabarns: L, static-exchange dipole length; V, static-exchange dipole velocity; $\bigcirc$, numerical results of Norcross (Ref. 33).

The dipole length cross section gives better agreement with Norcross results than does the velocity form. In general neither the dipole-length nor dipole-velocity form seems to give more reliable static-exchange results.

V. CONCLUSIONS

We have presented a method for calculating static-exchange electron–molecular-ion scattering wave functions. The method should be directly applicable to molecular systems. In e^--He^+ scattering, the numerical evaluation of the exact Schwinger variational expression gives extremely accurate phase shifts with small basis sets. In molecular systems, the numerical integration of the matrix elements, $\langle \alpha | U^s G^{c\,(P)} U^s | \beta \rangle$ may become extremely length. In this case, the approximate Schwinger expression with a large basis set inserted around $G^{c\,(P)}$ may be a more economical procedure. As presented here, the approximate Schwinger method yields a single center expansion of the scattering amplitude. This allows analytic averaging over target orientation. Both the exact Schwinger method and the approximate Schwinger method, with insertion in the denominator, can be used to compute accurate numerical scattering wave functions. These wave functions correspond to K matrices which are variationally stable.

Accurate static-exchange wave functions can be utilized in various distorted-wave approximations. In the example presented in this paper, these wave functions can be used in the calculation of the photoionization cross section of helium, even when the scattering basis set is of very modest size. Another use for electron-ion scattering wave functions is in the study of electron-impact ionization.

The application of the Schwinger variational principle to molecular systems is in progress.

TABLE X. Photoionization cross sections of the ground state of helium using the length form of the dipole operator, in megabarns. Comparison of $5p$ and $1p$ exact Schwinger cross sections with Coulomb wave results.

ΔE (eV)	Schwinger $\tilde{\sigma}(5p)$	Schwinger $\tilde{\sigma}(1p)$	Coulomb wave [a] σ^c
24.75	7.59	7.60	7.73
26.6	6.98	7.00	6.91
30.6	5.76	5.79	5.44
34.6	4.74	4.77	4.34
38.6	3.93	3.94	3.53
42.6	3.26	3.27	2.90
46.6	2.73	2.72	2.41

[a] The Coulomb wave cross section is obtained by using $\psi^{(P)}_{ll'm}(r) = \delta_{ll'}F_l(\gamma; kr)$ in Eqs. (60), (64), (66), and (67).

*Contribution No. 5981.

[1] B. I. Schneider, Phys. Rev. A 11, 1957 (1975).

[2] B. I. Schneider and P. J. Hay, Phys. Rev. A 13, 2049 (1976).

[3] M. A. Morrison and B. I. Schneider, Phys. Rev. A 16, 1003 (1977).

[4] T. N. Rescigno, C. W. McCurdy, and V. McKoy, Chem. Phys. Lett. 27, 401 (1974).

[5] T. N. Rescigno, C. W. McCurdy, and V. McKoy, Phys. Rev. A 10, 2240 (1974).

[6] T. N. Rescigno, C. W. McCurdy, and V. McKoy, Phys. Rev. A 11, 825 (1975).

[7] A. W. Fliflet, D. A. Levin, M. Ma, and V. McKoy, Phys. Rev. A 17, 160 (1978).

[8] A. W. Fliflet and V. McKoy, Phys. Rev. A 18, 2107 (1978).

[9] D. A. Levin, A. W. Fliflet and V. McKoy (unpublished).

[10] P. W. Langhoff, C. T. Corcoran, J. S. Sims, F. Weinhold, and R. M. Glover, Phys. Rev. A 14, 1042 (1976).

[11] C. T. Corcoran and P. W. Langhoff, J. Math. Phys. 18, 651 (1977).

[12] T. N. Rescigno, C. F. Bender, B. V. McKoy, and P. W. Langhoff, J. Chem. Phys. 68, 970 (1978).

[13] N. Padial, G. Csanak, B. V. McKoy, and P. W. Langhoff, J. Chem. Phys. 69, 2992 (1978).

[14] G. R. J. Williams and P. W. Langhoff, Chem. Phys. Lett. 60, 201 (1979).

[15] P. W. Langhoff, A. F. Orel, T. N. Rescigno, and B. V. McKoy, J. Chem. Phys. 69, 4689 (1978).

[16] J. M. Blatt and J. D. Jackson, Phys. Rev. 76, 18 (1949).

[17] R. G. Newton, *Scattering Theory of Waves and Particles* (McGraw-Hill, New York, 1966), p. 431.

[18] S. K. Adhikari and I. H. Sloan, Phys. Rev. C 11, 1133 (1975); see also W. H. Miller, J. Chem. Phys. 50, 407 (1969).

[19] M. E. Riley and D. G. Truhlar, J. Chem. Phys. 65, 792 (1976).

[20] M. Cohen and R. P. McEachran, Proc. Phys. Soc. 92, 37 (1967).

[21] M. J. Seaton, Comments At. Mol. Phys. 1, 184 (1970).

[22] T. N. Rescigno, J. Chem. Phys. 66, 5255 (1977).

[23] A. W. Fliflet and V. McKoy, Phys. Rev. A 18, 1048 (1978).

[24] M. Rotenberg, R. Biyins, N. Metropolis, and J. K. Wootin, *The 3-j and 6-j Symbols* (MIT, Cambridge, Mass., 1959), p. 6.

[25] S. Huzinaga, J. Chem. Phys. 42, 1293 (1965).

[26] D. K. Watson and V. McKoy, Phys. Rev. A (to be published).

[27] I. H. Sloan, Proc. R. Soc. A 281, 151 (1964).

[28] N. F. Mott and H. S. Massey, *The Theory of Atomic Collisions* (Oxford, London, 1965), p. 559.

[29] E. McGreevy and A. L. Stewart, J. Phys. B 10, L527 (1977).

[30] J. A. R. Samson, Adv. Mol. Phys. 2, 177 (1966).

[31] H. P. Kelly, Chem. Phys. Lett. 20, 547 (1973).

[32] M. Cohen and R. P. McEachran, Proc. Phys. Soc. 92, 37(1967); 92, 539 (1967).

[33] D. W. Norcross, J. Phys. B 4, 652 (1971).